Plasmonics
https://doi.org/10.1007/s11468-024-02294-5

RESEARCH

Gold Nanoparticles Biosynthesis Through Green Synthesis Mediated by Leaf Extract from *Diospyros Kaki* L. (Persimmon) Using the Microwave Extraction Method

Gönül Serdar[1]

Received: 29 January 2024 / Accepted: 5 April 2024

Abstract

The objective of this study was to prepare metallic gold nanoparticles (AuNPs) from the *Diospyros kaki* L. (persimmon) leaf (DKL) extract, which was grown in the Trabzon province of Türkiye, using microwave extraction. Separate additions of 0.1 and 0.5 mL DKL extract were made to the 0.5 mM $HAuCl_4.3H_2O$ solution while the heater was kept at 25 °C and stirring continuously. In this method, UV-Vis spectroscopy (300–800 nm) absorption measurements were performed on extracts of *Diospyros kaki* L. leaves at different time intervals (10, 20, 30, 60, 120, and 1440 min). Green chemistry principles were utilized in the preparation of gold nanoparticles (AuNPs), which were characterized by UV–visible, X-ray diffraction (XRD), transmission electron microscopy (TEM), Fourier-transform infrared spectroscopy (FTIR), and Zetasizer. FTIR analysis can be used to determine the various functional groups that were synthesized in the gold (Au) nanoparticles. Based on the AuNPs' XRD peaks, the average crystallite size was determined to be 25.99 nm. Zetasizer study results showed that the average particle size of Au nanoparticles produced by microwave extraction in an aqueous medium was 45.44 ± 1.095 nm, the zeta potential (ZP) was -16.9 mV ± 1.19, and the polydispersity index was 0.316 ± 0.009. The UV-Vis absorption spectra of the AuNP solutions were stable for approximately 2.5 to 3 months when they were kept in a refrigerator.

Keywords *Diospyros kaki* L. (persimmon) leaf · AuNPs · Microwave-assisted extraction · TEM · Zetasizer

Abbreviations

Au	Gold
NPs	Nanoparticles
AuNPs	Gold nanoparticles
DK	*Diospyros Kaki* L.
DKL	*Diospyros Kaki* L. leaves
PEG	Polyethylene glycol
PEG-200	Polyethylene glycol-200
SPR	Surface plasmon resonance
FTIR	Fourier transform infrared spectroscopy
XRD	X-ray diffraction
TEM	Transmission electron microscopy
DLS	Dynamic light scattering
ZP	Zeta potential

✉ Gönül Serdar
gonulserdar@ktu.edu.tr

[1] Department of Central Research Laboratory, Karadeniz Technical University, 61080 Trabzon, Turkey

Introduction

Nanoparticles (NPs), with sizes ranging from 1 to 100 nm, have been employed extensively in a variety of fields for decades [1, 2]. The components that green nanotechnology, which is a subset of nanotechnology, discloses at the molecular level, have recently received a lot of attention. Due to their widespread usage in treating a wide range of illnesses in medicine and other fields, these products continue to be a growing subject of study [3]. The physical and chemical characteristics of nanoparticles (NPs) are superior. NPs' exceptional qualities include their resistance to high-temperature changes in addition to their vast surface areas [4]. Particularly, nanometals like gold (Au), silver (Ag), and titanium (Ti) are used in fields like drug delivery systems, biological labeling, and optical devices. Some processes, like the synthesis and stability of metal nanoparticles (NPs), also receive a lot of attention in this area [5]. The usage of NPs in medicinal applications, the cosmetics and food industries, bioremediation research, and other fields makes them valuable materials as well [6, 7]. Different methods are used

Published online: 29 April 2024

to obtain metallic NPs. Among these methods, synthesis by biological methods has some advantages. Among these are advantages such as being eco-friendly, nominal energy, and cost-effective, as it does not contain toxic chemicals in the synthesis stages [8].

NPs can be produced by a variety of techniques, including chemical, mechanical, and biologic methods. While pure and well-defined nanoparticles can be effectively produced by mechanical and chemical means, capping agents are required to stabilize the size. The chemicals utilized for this purpose (stabilization) are hazardous and result in byproducts that are not environmentally friendly. It is necessary to employ a non-toxic strategy in order to resolve this problem. Thus, for this goal, green nanotechnology is employed [9, 10].

Gold nanoparticles (AuNPs) have recently gained popularity in biological applications such as drug delivery, antibacterial, and anti-cancer agents Dhandapani et al. [11]. The therapeutic drug delivery mechanism of AuNPs includes the control of immunological and anti-inflammatory responses. These mechanisms point to potential uses of AuNPs as "drugs" to treat various skin conditions [12]. Due to their biocompatibility, adaptability in size and surface chemistry, and unique plasmonic property, AuNPs are now recognized as a hot topic in the realm of nanosystem research and usage for topical drug administration [13]. For the environmentally benign production of AuNPs, biosynthesis techniques utilize naturally occurring metabolites from plants and microorganisms such as bacteria, fungus, and algae [14, 15]. The plant extract was utilized to create NPs [16] that have been shown to be more promising in terms of bioactivity and biocompatibility than those created using inorganic methods [17].

In the synthesis, biological reduction, and stabilization of metal nanoparticles, these phytochemicals are crucial. Additionally, it is believed that phenolic substances such as tannins, phenolic acids, and flavonoids contribute to the reducing or antioxidant properties of medicinal plants. These phenolic compounds function as hydrogen donators, reducing agents, singlet oxygen quenchers, and metal chelating agents because of their redox activity [18]. For stable and regulated size nanoparticle production, green synthesis is recommended. Additionally, there is less chance of pollution with green synthesis of nanoparticles [19, 20]. The nanoparticles are stabilized by biological material components that surround them [21]. In addition, the plant extract's secondary metabolites simultaneously stabilized and capped the zero-valent species of Au^0, leading to the synthesis of AuNPs [22]. Researchers have demonstrated that the majority of the chemicals listed above, which are responsible for the production of nanoparticles, are ecologically beneficial based on the results of numerous studies [23]. PEG (polyethylene glycol) is a synthetic, water-soluble, biocompatible polymer that is typically used in biomedical applications. Its main purpose is to coat nanoparticles in order to improve their penetration and dispersion in aqueous solutions.

Diospyros kaki L. (persimmon) is mostly grown in Eastern Asia, which includes Japan, China, and Korea and can be grown as well in Azerbaijan, India, Türkiye, Spain, USA, and Brazil [24]. Concerning the amount and value to economy, its fruit is regarded as one of the significant. There has been an increase in curiosity about the chemical and bioactive components of *Diospyros kaki* L. (DK) fruit recently. There have been numerous researches on the effects of DK vegetables and the substances they contain on human health. Carbohydrates, organic acids, phenolic molecules, carotenoids, and tannins make up the majority of DK fruit's ingredients and provide the fruit its anti-oxidant, anti-cancer, and pharmacological effects. Additionally, it contains a number of macro and micronutrients with high bioavailability [25]. The leaves of persimmon trees are valuable as ingredients for functional foods, medicines, and nutraceuticals since they are deciduous. Numerous bioactive substances, including caffeine, polysaccharides (cellulose, hemicelluloses, and lignins), phenolics (flavonoids), terpenoids, carotenoids (kryptoxanthin), amino acids, vitamin C, minerals, and chlorophylls, are found in persimmon leaves. Specifically, the leaves have a high concentration of phenolic compounds, such as kaempferol, proanthocyanidins, flavonolglucosides, myricitrin, quercetin, and isoquercetin, which have anti-inflammatory, antidiabetic, anti-cancer, anti-allergic, and vasorelaxant properties [24, 26–28]. Utilizing high-performance liquid chromatography–quadrupole time of flight–mass spectrometry (HPLC-QTOF-MS) in negative ion mode, Huang et al. [29] identified 32 compounds in persimmon leaves. The major compounds were hyperoside, quercetin, kaempferol, myricetin, trifolin, vitexin, astragalin, 19α, 24-dihydroxy ursolic acid, barbinervic acid, and pomolic acid. Both the fruit and the leaves of the DK are said to have significant biological benefits, such as anti-inflammatory properties, defense against atherosclerosis, a decrease in cholesterol levels, resistance to free radicals, protection against diabetes, cancer treatment, and cancer prevention [11].

In order to minimize the energy required for the synthesis of nanoparticles, underutilized biological resources have been investigated recently. These resources help reduce the metal ion to its equivalent nanoparticles at room temperature since they include phytochemicals [30]. In the literature, the biosynthesis of gold nanoparticles from the fruit part of *Diospyros kaki* L. has mostly been reported [11, 31, 32]. According to the information obtained by researching the literature so far, gold nanoparticles have not been synthesized by the green synthesis method from *Diospyros kaki* L. leaf

containing phenolic compounds collected from Trabzon city of Türkiye, and their characterization has not been studied. For this reason, it was aimed to collect *Diospyros kaki* L., an economically valuable plant, from Trabzon, obtain its extracts with laboratory microwaves, produce gold nanoparticles by the green method, and characterize it with XRD, Zetasizer, TEM, and FTIR in this study.

Materials and Methods

Extraction of *Diospyros kaki* L. Leaf

The leaves of *Diospyros kaki* L. were gathered from located in Trabzon province, Turkey. From their natural habitat in Trabzon, representative samples of *Diospyros kaki* L. leaves were gathered. Prof. Dr. Salih Terzioğlu verified the taxonomic identity of the plant material and then the plant material was added to the Herbarium of the Department of Forest Engineering Faculty at Karadeniz Technical University in Trabzon, Türkiye (KATO:19479). To get rid of any waste and pollutants, leaves were washed several times in deionized water. The leaves were then shred and let to dry. Then, to produce a fine powder, the dried leaves were ground up in a stainless steel mixer. The 10 g of *Diospyros kaki* L. leaves were shaken in 100 mL of water for 300 min in a shaker. They were then put in the flask of a 600-W microwave (Milestone Start S Microwave, USA), heated to 40 °C, extracted for 6 min, and cooled. All of the chemicals employed in the synthesis of AuNPs were of analytical grade, and the filtrate was collected.

DKL-AuNPs Biosynthesis

For the synthesis of DKL-AuNPs, a 0.5 mM metal solution was made using $HAuCl_4.3H_2O$ (99.9%, Sigma-Aldrich). Firstly, 20 mL of the $HAuCl_4.3H_2O$ (0.5 mM) aqueous solution was mixed with 0.1 mL and 0.5 mL volume of DKL extract solution at 25 °C under continuous stirring. The stabilizing agent polyethylene glycol (PEG-200, 1%), after the optimal parameters were identified, was used to produce the nanoparticles. Every procedure was run three times. The way allowed for different minutes to witness the color shift. Based on the color shift, samples from the reaction media were extracted. A common sign that colloidal AuNP is forming in the solution is this shift in hue. In this optimized method, such as varying the amount of DKL extract and reaction parameters like concentration, time, and volume were investigated. UV-Vis spectroscopy was used to monitor the AuNPs production kinetics. Following the end of the reaction, the pellet was again suspended after the resulting DKL-AuNPs were centrifuged three times for 15 min at 10,000 rpm. DKL-AuNPs were stored at 4 °C in anticipation of future studies. The metal ion reduction was seen using ultraviolet-visible spectroscopy at a wavelength of 300–800 nm.

DKL-AuNPs Characterization

An important technique for evaluating the creation and stability of metal nanoparticles in aqueous solutions is UV-Vis spectroscopy, which is used in the DKL-AuNPs characterization procedure. *Diospyros kaki* L. (persimmon) leaf extracts at different time intervals were used by UV-Vis spectroscopy (300 – 800 nm) absorption measurements (Shimadzu, Japan) in this method. As a result of these measurements, SPR bands of Au nanoparticles were formed and characteristic plasmon resonance peaks around 500–600 nm were determined, indicating the formation of gold nanoparticles. The sharp narrow-shaped band is evidence of both spherical and homogeneous distribution of gold nanoparticles [33]. The stability criterion requires that the highest absorbance value remain constant when samples collected at different times are examined [34]. The different functional groups in the produced AuNPs can be identified via FTIR analysis. It offers details on a molecule's structure, which are usually learned through. Using Fourier-transform infrared (FT-IR) (PerkinElmer Frontier) spectroscopy in the range of 4000–550 cm^{-1}, the organic compounds encapsulated on the exterior of the DKL-AuNPs were categorized. The crystal sizes and patterns of the particles produced during the synthesis were examined using an XRD. With the use of X-ray data in the 10°–90° range, the XRD pattern of the synthesized DK-AuNPs sample was obtained utilizing an X-ray diffractometer (XRD, Panalytical X'Pert3 Powder). TEM micrographs captured using the Hitachi HT-7700 instrument were utilized to examine the morphological characteristics of the generated AuNPs. Furthermore, the morphological structure was examined using the data obtained from TEM images. The surface charges and size distributions of the produced DKL-AuNPs were measured using the zeta potential distribution device. Using a zeta size analyzer, zeta potentials, polydispersity indices (PI), and average particle sizes of Au nanoparticles are calculated using the DLS technique (Malvern Zetasizer Nano ZSP), a light source of a He–Ne laser with a wavelength of 633 nm, a maximum power of 10 mW, and a maximum power of 100 VA.

Statistical Analysis

Every experiment is carried out thrice, dependent on the determined analytical method, and the mean ± standard deviation (SD) ($n = 3$) was employed.

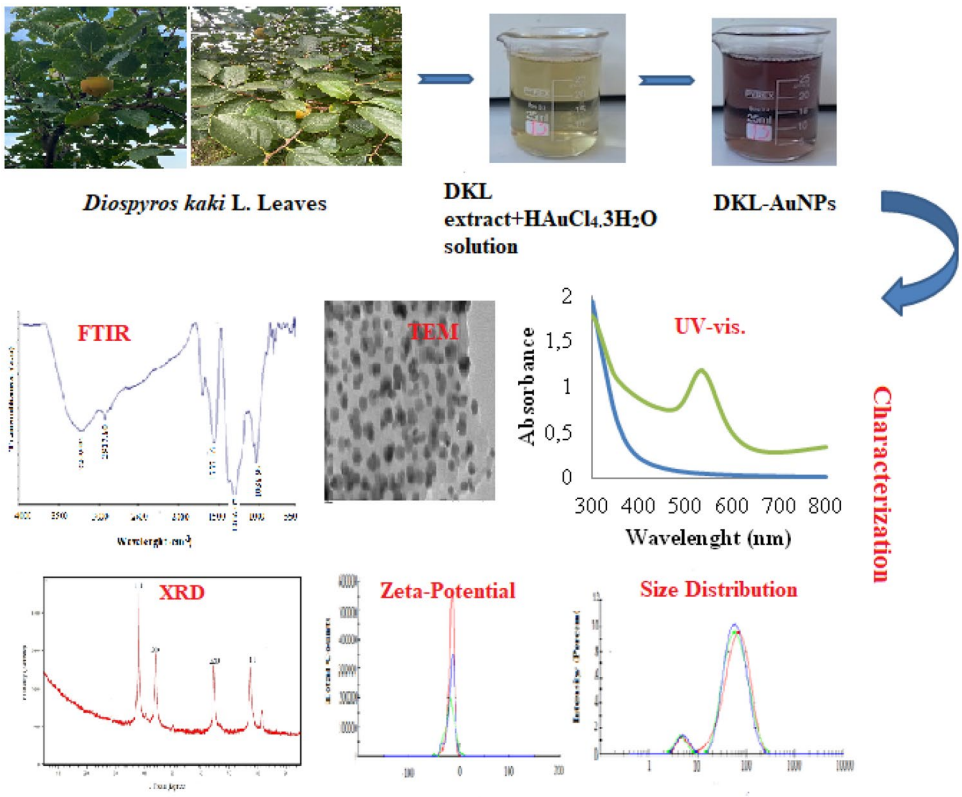

Fig. 1 A schematic representation of the green synthesis and characterization of DKL-AuNPs

Results and Discussion

Characterization of DKL-AuNPs

Consequently, a shortened process for the phytosynthesis of DKL-AuNPs employing an aqueous extract of *Diospyros kaki* L. (persimmon) leaves is shown in Fig. 1.

As such, the use of chemicals was unnecessary. It is hypothesized that these phytoconstituents function as both a stabilizing and a reducing agent simultaneously. First, reduced gold ions into a metallic or zero-valent form of gold (AuNPs) are extracted from the leaves of *Diospyros kaki* L. (persimmon).

UV–Visible Spectroscopy

UV–visible spectroscopy is used to identify surface plasmonic resonance, which is the distinct peak at a wavelength where a light source produces excitation [35, 36]. Surface plasmon resonance (SPR) bands are specific to most metallic nanoparticles [35]. Furthermore, the form and location of the SPR peak are often determined by the size and shape of the NPs.

When $HAuCl_4.3H_2O$ was mixed, the color of the extract quickly changed from light yellow to purple; this shows the synthesis of AuNPs (Fig. 2a, b). In UV-Vis spectroscopic examination of the produced DKL-AuNPs solution in the wavelength range of 300–800 nm, a strong surface plasmon peak at 534 nm was obtained, confirming the synthesis of DKL-AuNPs. However, the DKL solution did not exhibit any absorption peak between 300 and 800 nm (Fig. 2c).

Figures 3 and 4 display the UV-Vis spectra of Au nanoparticles that were produced at 25 °C using 0.1–0.5 mL DKL extract and 0.5 mM $HAuCl_4.3H_2O$ solutions. This consists of the metal salt (Au) and the synthesis time concentration and the amount of DKL extract during the biosynthesis of DKL-AuNPs.

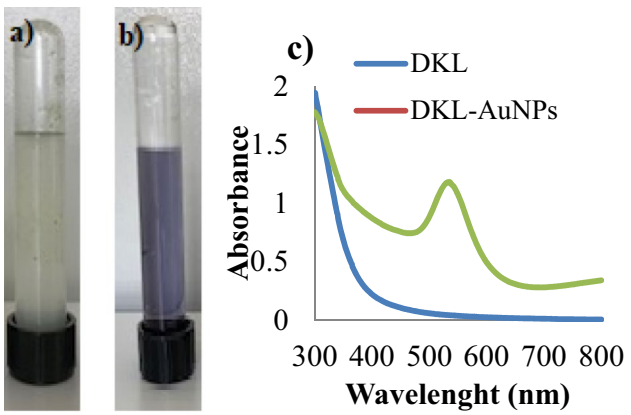

Fig. 2 Biosynthesis of DKL-AuNPs: **a** initial color of DKL solution, **b** color change from pale yellow to purple after incubation at room temperature, and **c** UV-Vis spectra of DKL and DKL-AuNPs

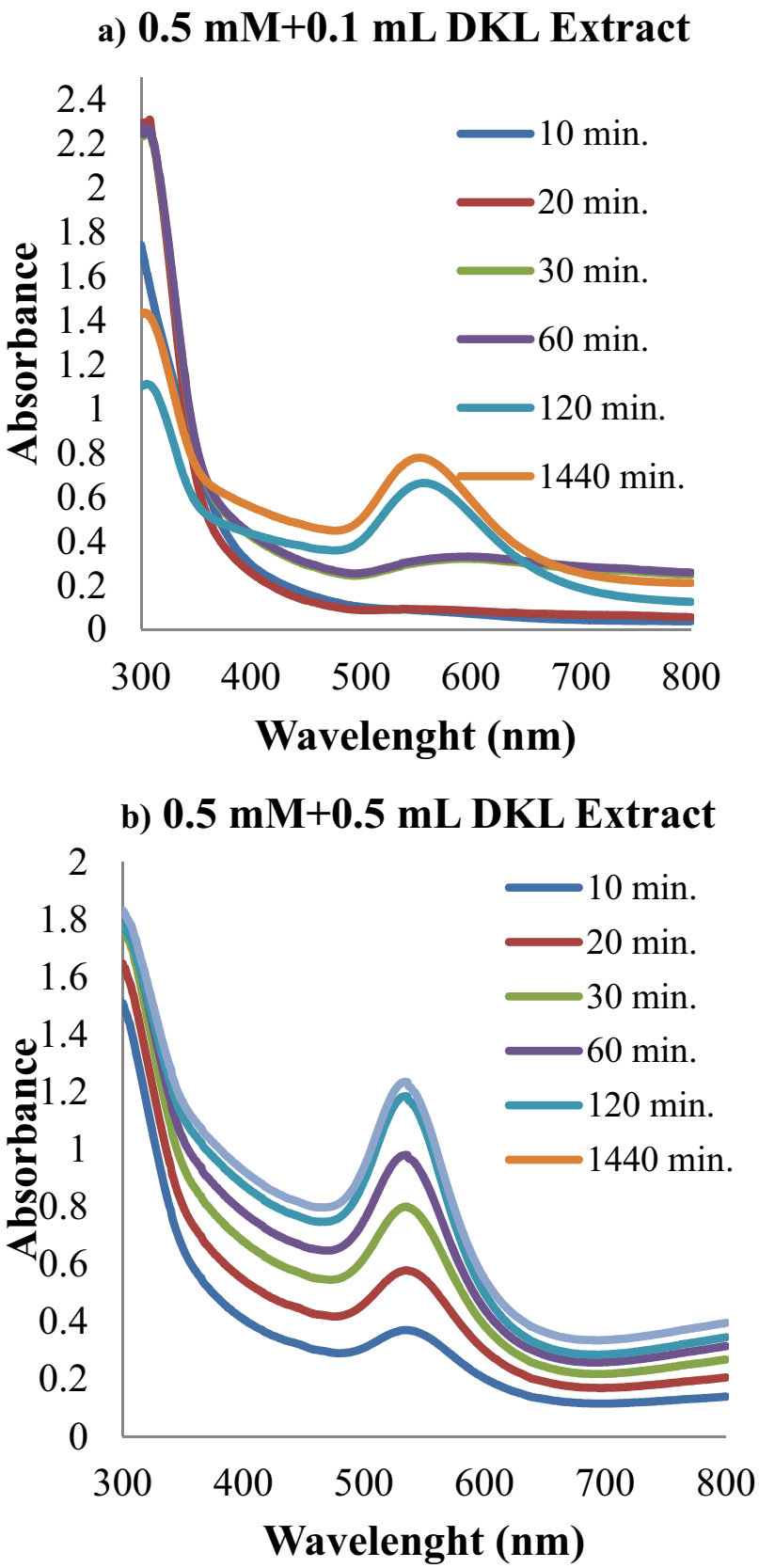

Fig. 3 UV-Vis spectra of Au nanoparticles synthesized at 25 °C with 0.5 mM $HAuCl_4.3H_2O$ and in different volume of DKL extract (**a** 0.1 mL, **b** 0.5 mL)

In Fig. 3a, a specific resonance band of DKL-AuNPs was first produced at 555 nm after 120 min. AuNPs were successfully produced at 540 nm after 10 min, and the band peaked after two hours with 0.5 mL of DKL extract as shown in Fig. 3b, and the band peaked after 2 h. Following a 10-min time span, at 540 nm for 0.5 mM of $HAuCl_4.3H_2O$, the SPR peaks emerged and after 2 h of reaction, the peaks gradually moved to 534 nm (Fig. 3b). Similarly, the addition of PEG-200 (1%), a stabilizing substance presented during synthesis. The SPR peaks appeared at 531 nm at a 10-min interval, and after 2 h of processing, they progressively shifted to 533 nm (Fig. 4b). As a result, an SPR peak characteristic of AuNPs at 534 nm, as depicted in Fig. 3b, validated the successful phytosynthesis of DKL-AuNPs utilizing 0.5 mL of the aqueous extract of *Diospyros kaki* L. (persimmon) leaves in this study. Nanoparticle production was higher in 0.5 mL extract volume (Figs. 3b and 4b). A high extract volume (0.5 mL) increased the number of nanoparticles. It is possible that PEG-200 (1%) (Fig. 4a, b) restricted the production of nanoparticles in some way. There must be restrictions on bioactive compounds having lowering effects [33, 37]. The stability of the produced nanoparticles is also influenced by storage duration. Even after 75 days, as can be shown in Fig. 5, there was no discernible change in the UV-Vis spectra of DKL-AuNPs, suggesting that they were stable. However, a slight decrease in the spectrum was observed after 90 days and DKL-AuNPs were stable for up to 2.5–3 months (Fig. 5). Based on these findings, it can be concluded that AuNPs have remarkable dispersion stability against aggregation due to the negative biomolecules derived from DKL extract.

In the literature, Dhandapania et al. [11] and Huo et al. [32] produced gold nanoparticles from *Diospyros kaki* L. fruit under various conditions. Dhandapani et al. [11] optimized reaction parameters such as pH, temperature, and time by using different concentrations of gold salt and DK fruit extracts to biosynthesize DK-AuNPs. They carried out the synthesis at 50–80 °C temperatures, 5–20-min reaction time spans, DK concentrations of 6–9 mg/mL, and $HAuCl_4.3H_2O$ concentrations of 1–5 mM. Dhandapani et al. [11] found maximum peak was 547 nm of optimized DK-AuNPs. Huo et al. [32] boiled a mixture of 2 g of persimmon powder and 200 mL of deionized water for 5 min. To examine the impact of $HAuCl_4.4H_2O$ concentration on the synthesis of AuNPs, 10 mL of persimmon extract was mixed with 50, 100, 150, and 200 mL of $HAuCl_4.4H_2O$ (10 mM). These mixes were then allowed to incubate at room temperature. Furthermore, the impact of reaction temperature was investigated through the incubation of the extract and $AuCl_4.4H_2O$ mixes at 30, 40, 50, 60, and 70 °C. The UV-Vis spectra were used to track the progress of the synthesis. Huo et al. [32] reported that when adding $HAuCl_4.4H_2O$, the extract's color quickly transformed from pale orange to purple, resulting in the formation of gold nanoparticles, and after 10 min, SPR peaks were observed at 532, 533, and 546 nm. There is no article in the literature showing the biosynthesis of gold nanoparticles at 25 °C from DKL extract obtained using the method, like in this one.

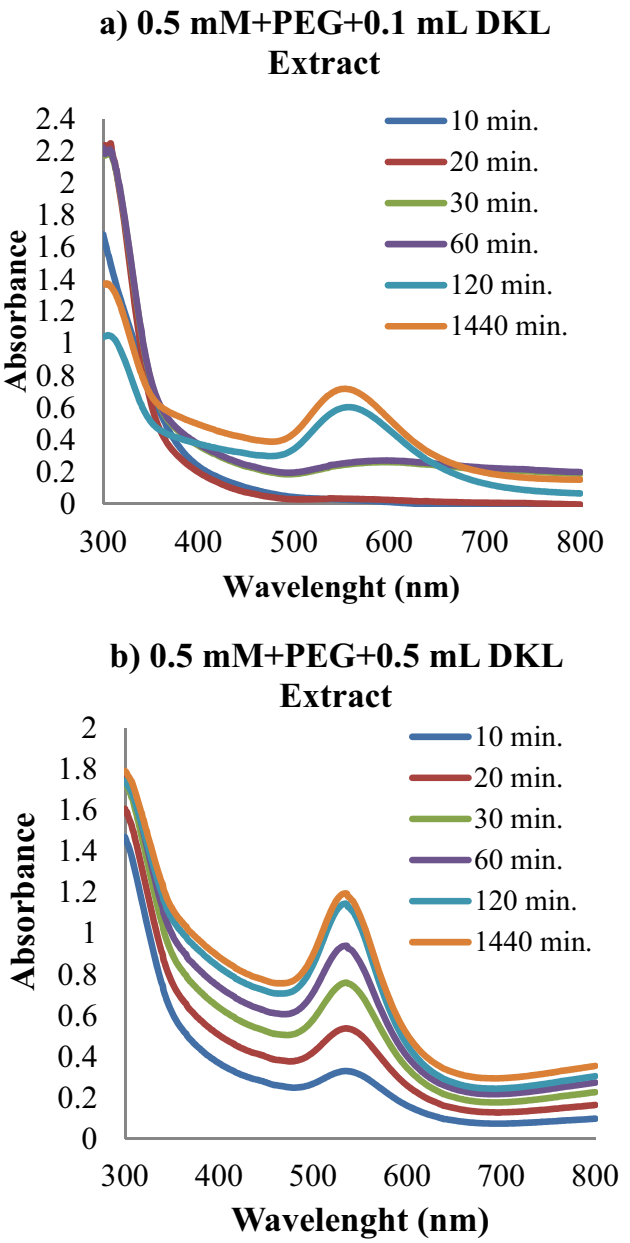

Fig. 4 UV-Vis spectra of Au nanoparticles synthesized at 25 °C with 0.5 mM $HAuCl_4.3H_2O$ and in different volume of DKL extract and in the presence of PEG (**a** 0.1 mL, **b** 0.5 mL)

TEM Analysis

The TEM images in Fig. 6 verify the production of AuNPs (0.5 mM, 0.5 mL, no PEG-200, 25 °C), and these images

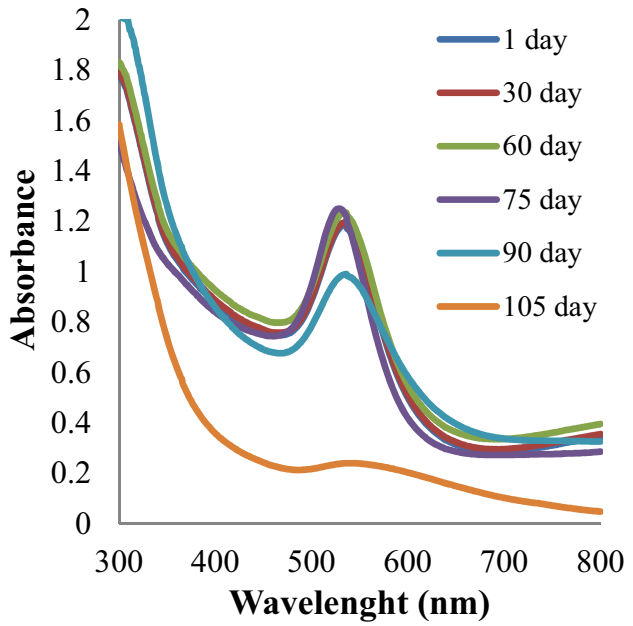

Fig. 5 UV-Vis spectra of DKL-AuNPs at different storage intervals

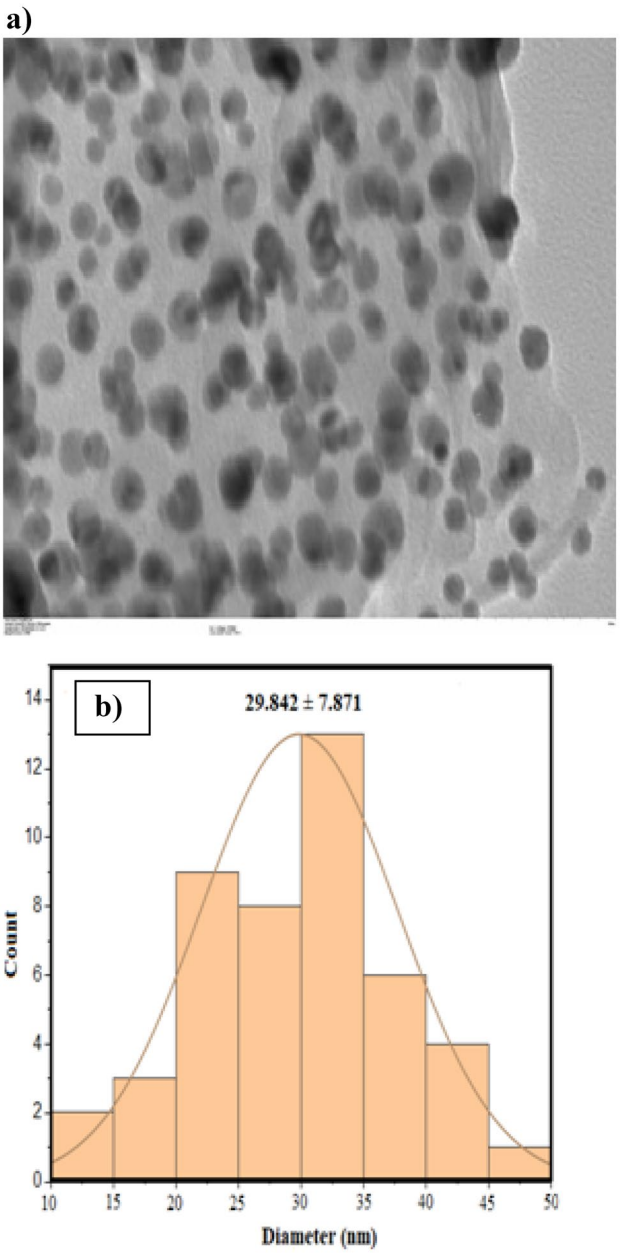

Fig. 6 **a** TEM image (100 nm) of Au nanoparticles synthesized at 25 °C with 0.5 mM $HAuCl_4.3H_2O$ with 0.5 mM $HAuCl_4.3H_2O$ and 0.5 mL DKL extract. **b** Size distribution of AuNP

show that the structure of the spherical gold nanoparticles is consistent with the shape of the resonance band in the UV-Vis spectrum.

Based on the data presented in Fig. 6a and b, it was determined that the average particle size of DKL-AuNPs was approximately between 14.907 and 46.021 nm. Depending on the TEM images, the DKL-AuNPs had a mean size of 29.842 ± 7.871 nm (Fig. 6b). Dhandapani et al. [11] reported 23.42 ± 12.6 nm based on TEM image results of DK-AuNPs size. Huo et al. [32] reported that the isotropic growth of AuNPs had no significant effect on the size of AuNPs, despite the increase in temperature (50, 60, and 70 °C). Huo et al. [32] reported TEM images of synthesized AuNPs 12 ± 5 nm, 16.5 ± 8.4, and 30.7 ± 15.8 nm size, respectively, at 0.5, 1.0, and 1.5 mM concentrations of $HAuCl_4.4H_2O$. The size of DKL-AuNPs in this study was found to be compatible with the size of DK-AuNPs in the literature by Huo et al. [32] and Dhandapani et al. [11].

FT-IR Analysis

An open spectrum library for bioactive compounds and the FT-IR spectrum database was used to evaluate the samples' FT-IR spectra and determine their chemical linkages.

Different patterns were seen in the samples (Fig. 7). FTIR measurement provided additional evidence that potential functional groups in the persimmon extract were engaged in the synthesis process. The functional groups on the surface of the biosynthesized AuNPs obtained from the extract of persimmon leaves, as evidenced by the lack of significant difference between the spectra of the extract of persimmon leaves and the AuNPs that were biosynthesized utilizing the extract of this leaf (Fig. 7 a, b). The peaks at 3210.46 cm^{-1} and 3209.94 cm^{-1}, respectively, are the result of the phenolic and aliphatic hydroxyl groups in DKL and DKL-AuNPs. The protein's methylene group's C-H stretch was linked to the bands at 2919.94 cm^{-1} in DKL and 2917.80 cm^{-1} in DKL-AuNPs. The presence of the C–C bond in benzene may be responsible for the peak in DKL at 1545.04 cm^{-1} and the peak in DKL-AuNPs at 1552.16 cm^{-1}. The stretching

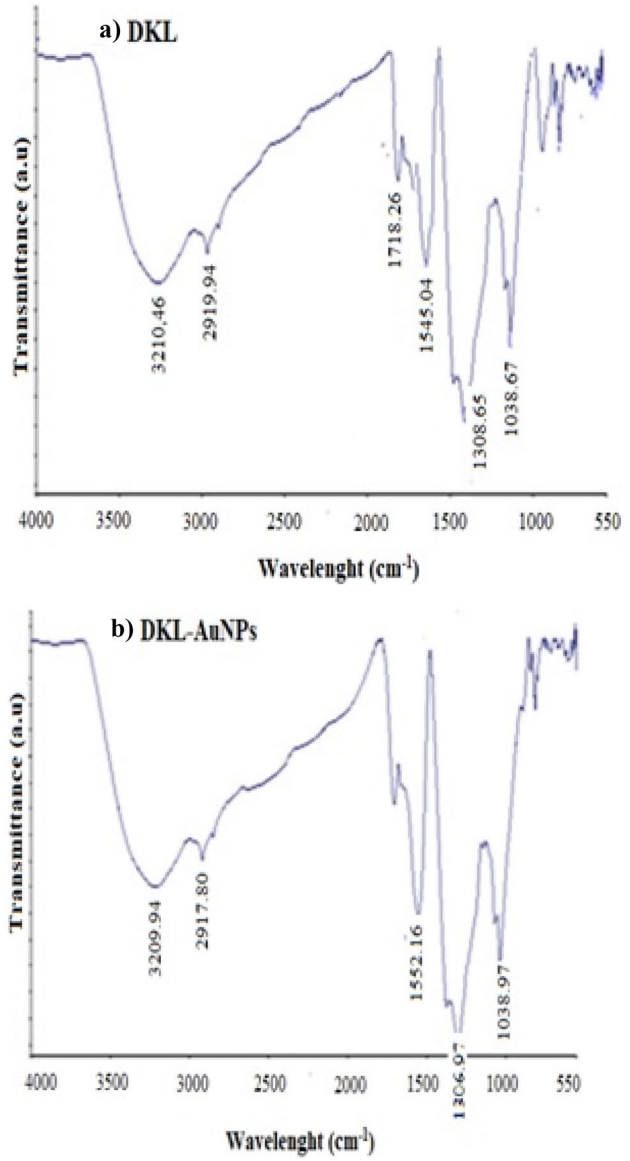

Fig. 7 FT-IR spectra of *Diospyros kaki* L. leaves (**a**) and DKL-AuNPs (**b**)

vibrations of C-H and C = C may be associated with the peaks located at 1552.16 and 2917.80 cm^{-1} (Fig. 7b) [32, 38]. The spectra of persimmon extract and the biosynthesized AuNPs utilizing persimmon extract were not significantly different, according to reports by Huo et al. [32] and Dhandapania et al. [11].

XRD Analysis

The XRD pattern verified the crystalline structure of DKL-AuNPs.

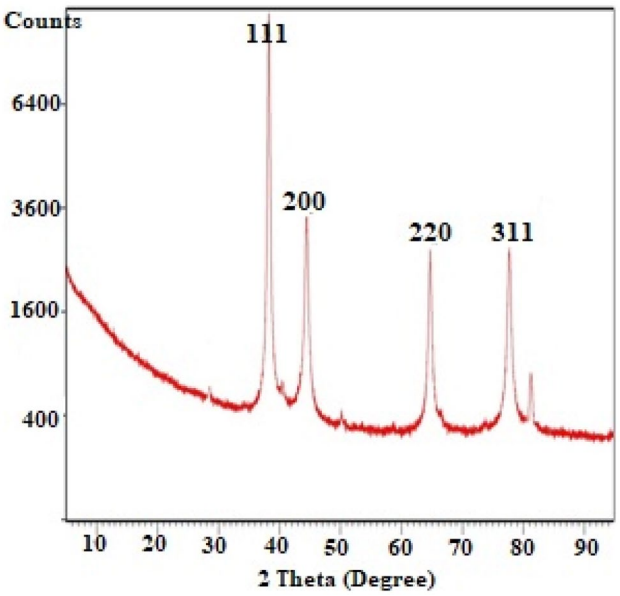

Fig. 8 XRD pattern of DKL-AuNPs

Figure 8 shows that distinct diffraction peaks of AuNPs were found at 38.2645°, 44.3936°, 64.6392°, and 77.6093°, which correspond to the lattice planes (111), (200), (220), and (311). Moreover, the (111) plane was the preferred growth direction of the green-produced DKL-AuNPs. The results obtained were in compliance with JCPDS 04-0784, the specified standards for crystalline gold. The average crystallite size of DKL-AuNPs was calculated using the Scherrer formula, and it was found to be approximately 25.99 nm, which was in close proximity to the size range (29.842 nm) reported by TEM spectroscopy. Huo et al. [32] and Dandapani et al. [11] determined four different results from XRD of DK-AuNPs. Huo et al. [32] found the diffraction peaks corresponding to the (111), (200), (220), and (311) planes at 38.10, 44.24, 64.47, and 77.38, and Dandapani et al. [11] found the diffraction peaks at 38.14, 44.31, 64.55, and 77.59 and reported that they found it compatible with JCPDS file No. 04-0784. The results of this study were found to be compatible with the XRD results of Huo et al. [32] and Dandapani et al. [11].

Zeta Potential and Particle Size

The microwave-extracted Au nanoparticles in Fig. 9a and b had an average particle size of 45.44 ± 1.095 nm in an aqueous solution, a zeta of 0.45 ± 0.011, and a polydispersity index of 0.316 ± 0.009. Using a zeta analyzer, the stability and surface charge of green-produced DKL-AuNPs were examined. This method is frequently used to assess the dispersion stability of nanoparticles [35, 39]. Zeta potential

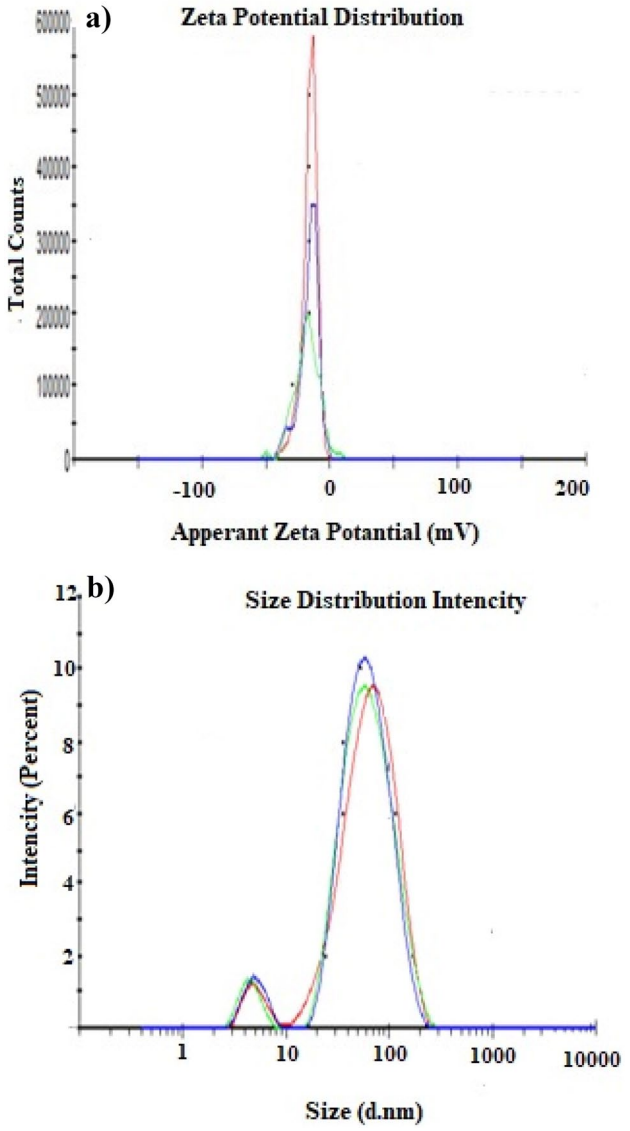

Fig. 9 **a** Zeta potential and **b** size distribution of Au nanoparticle synthesized at 25 °C with 0.5 mM $HAuCl_4.3H_2O$ and 0.5 mL DKL extract

for DKL-AuNPs was − 16.9 mV ± 1.19 (Fig. 9), indicating that DKL-AuNPs were stable. Nanoparticles become more stable as the zeta potential value decreases [40]. Because DKL-AuNPs are capped with negatively charged phytoconstituents that create repulsion (dispersion) among them and promote their stability, they exhibit a negative zeta potential. DLS analysis demonstrates how size distribution varies with conjugated diameter or hydrodynamic size in particles that are colloidal; hence, the sizes are frequently higher than those found by TEM analysis [11]. Huo et al. [32] reported when 0.5, 1.0, 1.5, and 2.0 mM of $HAuCl_4.4H_2O$ were utilized as precursors, respectively, the resulting zeta potential values of AuNPs were − 24.1, − 23.2, − 23.3, and − 25.8 mV in literature. According to the result of this study, the average particle size of DKL-AuNPs in an aqueous solution (45.44 ± 1.095 nm) was founded higher than the average size of DKL-AuNPs (29,842 ± 7871 nm) of TEM image.

Conclusion

According to the results of this work, it can be concluded that gold nanoparticles can be produced from *Diospyros kaki* L. (persimmon) leaf extracts utilizing this method, which uses less energy overall. Utilizing of *Diospyros kaki* L. (persimmon) leaf aqueous extract as reducing and stabilizing agents, this study illustrated a biological process for the biosynthesis of DKL-AuNPs. Primary phytochemicals from *Diospyros kaki* L. (persimmon) leaf extracts are transformed into DKL-AuNPs by a plant-mediated process that is environmentally benign. The current work is the demonstrate a rapid, one-step, cost-effective, and environmentally friendly production of gold nanoparticles (DKL-AuNPs) utilizing the aqueous extract of *Diospyros kaki* L. (persimmon) leaf. The phytosynthesis of DKL-AuNPs using the investigated species' aqueous extract was deemed to be successful and efficient, as they were found stable for more than 2.5–3 months and evidenced by the formation of dark purple and sperical or elliptical. Furthermore, it can be said that the synthesis of DKL-AuNPs in the current study adheres to numerous green chemistry principles, including the use of renewable feedstocks, energy efficiency in design, and the avoidance of toxic solvents.

Acknowledgements The author acknowledges thanks to the Central Research Laboratories of Atatürk University and Karadeniz Technical University and Prof. Dr. Salih Terzioğlu.

Author Contribution G.S. wrote the main manuscript text, prepared figures, and reviewed the manuscript.

Funding There was no significant funding for this study.

Data Availability The author can provide the data utilized in this work reasonably requested, even though it is not publicly accessible at this time.

Declarations

Ethical Approval This report declares that no human or animal research is included.

Conflict of Interest The author declares no competing interests.

References

1. Cho NH, Kim YB, Lee YY, Im SW, Kim RM, Kim JW, Namgung SD, Lee HE, Kim H, Han JH (2022) Adenine oligomer directed synthesis of chiral gold nanoparticles. Nat Commun 13(1):1–10
2. Contini C, Hindley JW, Macdonald TJ, Barritt JD, Ces O, Quirke N (2020) Size dependency of gold nanoparticles interacting with model membranes. Commun Chem 3(1):1–12
3. Ramazanli VN, Ahmadov IS (2022) Synthesis of silver nanoparticles by using extract of olive leaves. Adv Biol Earth Sci 7(3):238–244
4. Syafiuddin A, Salim MR, Beng Hong Kueh A, Hadibarata T, Nur H (2017) A review of silver nanoparticles: research trends, global consumption, synthesis, properties, and future challenges. J Chin Chem Soc 64(7):732–756
5. Emmanuel R, Palanisamy S, Chen SM, Chelladurai K, Padmavathy S, Saravanan M et al (2015) Antimicrobial efficacy of green synthesized drug blended silver nanoparticles against dental caries and periodontal disease causing microorganisms. Mater Sci Eng C 56:374–379
6. Arroyo GV, Madrid AT, Gavilanes AF, Naranjo B, Debut A, Arias MT et al (2020) Green synthesis of silver nanoparticles for application in cosmetics. J Environ Sci Health 55(11):1304–1320
7. Khalilov R (2023) A comprehensive review of advanced nanobiomaterials in regenerative medicine and drug delivery. Adv Biol Earth Sci 8(1):5–18
8. Singh J, Mehta A, Rawat M, Basu S (2018) Green synthesis of silver nanoparticles using sun dried tulsi leaves and its catalytic application for 4-Nitrophenol reduction. J Environ Chem Eng 6(1):1468–1474
9. Shahzadi T, Sanaullah S, Riaz T, Zaib M, Kanwal A, Jabeen H (2021) Kinetics and thermodynamic studies of organic dyes removal on adsorbent developed from Viola tricolor extract and evaluation of their antioxidant activity. Environ Dev Sustain 23:17923–17941
10. Iravani S, Korbekandi H, Mirmohammadi SV, Zolfaghari B (2014) Synthesis of silver nanoparticles: chemical, physical and biological methods. Res Pharm Sci 9(6):385–406
11. Dhandapani S, Wang R, Hwang KC, Kim H, Kim YJ (2023) Enhanced skin anti-inflammatory and moisturizing action of gold nanoparticles produced utilizing *Diospyros kaki* fruit extracts. Arab J Chem 16(4):104551
12. Ko WC, Wang SJ, Hsiao CY, Hung CT, Hsu, Y.J.,& Chang, D.C. (2022) Pharmacological role of functionalized gold nanoparticles in disease applications. Molecules 27(5):1551
13. Chen Y, Feng X (2022) Gold nanoparticles for skin drug delivery. Int J Pharm 625:122122
14. Sanjeevram D, Xu X, Wang R, Puja AM, Kim H, Perumalsamy H, Balusamy SR, Kim YJ (2021) Biosynthesis of gold nanoparticles using Nigella sativa and Curtobacterium proimmune K3 and evaluation of their anticancer activity. Mater Sci Eng C 127:112214
15. Xu XY, Tran THM, Perumalsamy H, Sanjeevram D, Kim YJ (2021) Biosynthetic gold nanoparticles of Hibiscus syriacus L callus potentiates anti-inflammation efficacy via an autophagy dependent mechanism. Mater Sci Eng C 124:112035
16. Doan VD, Pham QH, Huynh BA, Nguyen AT, Nguyen TD (2021) Kinetic analysis of nitrophenol reduction and colourimetric detection of hydrogen peroxide based on gold nanoparticles catalyst biosynthesised from Cynomorium songaricum. J Environ Chem Eng 9(6):106590
17. Marcelino MY, Borges FA, Scorzoni L, de Lacorte Singulani J, Garms BC, Niemeyer JC, Guerra NB, Brasil GSAP, Mussagy CU, de Oliveira Carvalho FA (2021) Synthesis and characterization of gold nanoparticles and their toxicity in alternative methods to the use of mammals. J Environ Chem Eng 9(6):106779
18. Shahzadi T, Rehman S, Riaz T, Zaib M (2022) Eco-friendly synthesis of ZnO nanoparticles using cannabis sativa and assessment of its activities as efficient dyes removal and antioxidant agent. Int J Envıron Anal Chem 102(16):4738–4756
19. Shahzadi T, Anwaar A, Riaz T, Zaib M (2022) Sulfate and phosphate ions removal using novel nano-adsorbents: modeling and optimization, kinetics, isotherm and thermodynamic studies. Int J Phytoremedıatıon 24(14):1518–1532
20. Shafey AME (2020) Green synthesis of metal and metal oxide nanopar-ticles from plant leaf extracts and their applications: a review. Green Process Synth. 9(1):304–339
21. Nayak S, Sajankila SP, Rao CV (2018) Green synthesıs of gold nanoparticles from banana pıth extract and ıts evaluatıon of antıbacterıal actıvıty and catalytıc reductıon of malachıte green dyes. J Microbiol Biotech Food Sci 7(6):641–645
22. Wang M, Meng Y, Zhu H, Hu Y, Chang-Peng X, Chao X, Li W, Pan C, Li C (2021) Green synthesized gold nanoparticles using Viola betonicifolia leaves extract: characterization, antimicrobial, antioxidant, and cytobiocompatible activities. Int Nanomed J 16:7319
23. Pradeep M, Kruszka D, Kachlicki P, Mondal D, Franklin G (2021) Uncovering the phytochemical basis and the mechanism of plant extract-mediated eco-friendly synthesis of silver nanoparticles using ultra-performance liquid chromatography coupled with a photodiode array and high-resolution mass spectrometry. ACS Sustain Chem Eng 10(1):562–571
24. Hossain A, Shahidi F (2023) Persimmon leaves: nutritional, pharmaceutical, and industrial potential—a review. Plants 12:937
25. Matheus JRV, Andrade CJ, Miyahira RF, Fai AEC (2020) Persimmon (Diospyros Kaki L): chemical properties, bioactive compounds and potential use in the development of new products–a review. Food Rev 1–18:1733597
26. Las Heras RM, Quifer-Rada P, Andrés A, Lamuela-Raventós R (2016) Polyphenolic profile of persimmon leaves by high resolution mass spectrometry (LC-ESI-LTQ-Orbitrap-MS). J Funct Foods 23:370–377
27. Hossain A, Moon HK, Kim JK (2018) Effect of drying and harvest time on the physicochemical properties of the most common Korean persimmon leaves. Korean J Food Preserv 25:428–435
28. Hossain A, Moon HK, Kim JK (2018) Antioxidant properties of Korean major persimmon (Diospyros kaki) leaves. Food Sci Biotechnol 27:177–184
29. Huang SW, Wang W, Zhang MY, Liu QB, Luo SY, Peng Y, Sun B, Wu DL, Song SJ (2016) The effect of ethyl acetate extract from persimmon leaves on Alzheimer's disease and its underlying mechanism. Phytomedicine 23:694–704
30. Nayak S, Sajankila SP, Goveas LC, Rao VC, Mutalik S, Shreya BA (2020) Two fold increase in synthesis of gold nanoparticles assisted by proteins and phenolic compounds in *Pongamia* seed cake extract:response surface methodology approach. SN Appl Sci 2:634
31. Keskin C, Ölçekçi A, Baran A, Baran MF, Eftekhari A, Omarova S, Khalilov R, Aliyev E, Sufianov A, Beilerli A, Gareev I (2023) Green synthesis of silver nanoparticles mediated *Diospyros kaki* L. (Persimmon): determination of chemical composition and evaluation of their antimicrobials and anticancer activities. Front Chem. https://doi.org/10.3389/fchem.2023.1187808
32. Huo C, Khoshnamvand M, Liu P, Liu C, Yuan CG (2019) Rapid mediated biosynthesis and quantification of AuNPs using persimmon (*Diospyros Kaki* L.f) fruit extract. J Mol Struct 1178:366–374
33. Serdar G, Gül Kılınç G (2023) Microwave assisted production and characterization of gold nanoparticles using green tea and catechin extracts obtained by supercritical extraction method. Chem Papers 77(9):5155–5167
34. Jabir MS, Nayef UM, Abdulkadhim WK, Taqi ZJ, Sulaiman GM, Sahib UI et al (2021) Fe_3O_4 nanoparticles capped with PEG

induce apoptosis in breast cancer AMJ13 cells via mitochondrial damage and reduction of NF-κB translocation. J Inorg Organomet Polym Mater 31:1241–1259
35. Eltaweil AS, Fawzy M, Hosny M, Eltaweil AS, El-Monaem EMA, Fawzy M, Tamer TM, Omer AM (2022) Green synthesis of platinum nanoparticles using Atriplex halimus leaves for potential antimicrobial, antioxidant, and catalytic applications. Arab J Chem 15:103517
36. Zada S et al (2018) Biofabrication of gold nanoparticles by Lyptolyngbya JSC-1 extract as super reducing and stabilizing agents: synthesis, characterization and antibacterial activity. Microb Pathog 114:116–123
37. Sökmen M, Alomar SY, Albay C, Serdar G (2017) Microwave assisted production of silver nanoparticles using green tea extracts. J Alloys Compd 725:190–198
38. Karthik R, Chen SM, Elangovan A, Muthukrishnan P, Shanmugam R, Lou BS (2016) Phyto mediated biogenic synthesis of gold nanoparticles using Cerasus serrulata and its utility in detecting hydrazine, microbial activity and DFT studies. J Colloid Interface Sci 468:163–175
39. Tahir K, Nazir S, Ahmad A, Li B, Khan AU, Khan ZUH, Khan FU, Khan QU, Khan A, Rahman Au (2017) Facile and green synthesis of phytochemicals capped platinum nanoparticles and in vitro their superior antibacterial activity. J Photochem Photobiol, B 166:246–251
40. Shah R, Eldridge D, Palombo E, Harding I (2014) Optimisation and stability assessment of solid lipid nanoparticles using particle size and zeta potential. J Physical Sci 25(1):59–75